

Computational Models of Space: Isovists and Isovist Fields*

LARRY S. DAVIS† AND MICHAEL L. BENEDIKT‡

†Computer Sciences Department and ‡School of Architecture, The University of Texas at Austin, Austin, Texas 78712

Received April 5, 1979

A new computational model for space representation, called the isovist, is defined. Given a point x in a space P , the isovist at x , V_x , is the subset of P visible from x . Procedures for computing V_x for polygonal spaces are presented. Next, isovist fields are defined by associating a scalar measure of V_x at each point x in P . The architectural and computational significance of these fields is discussed. Finally, an analysis of computing small, sufficient sets of points is given. A set of points is sufficient if the union of the isovists of the points in the set is the entire space P . Sufficient sets are related to the endpoints of branches of the skeleton in the case of polygonal spaces.

1. INTRODUCTION

A central problem in image pattern recognition is the representation and analysis of form or shape. A significant amount of research has been devoted to developing shape representations for the purpose of recognition—e.g., Fourier models [1, 2], moment models [3], piecewise approximation [4-6]; see [7] for a more comprehensive review. Less effort has been devoted to developing models for describing the distribution of space within a (not necessarily simple) shape. We shall call the latter representations *space representations* to distinguish them from other shape representations. Some examples of space representations include work on the decomposition of shapes into primary convex subsets [8] and into symmetric pieces [9].

In this paper we describe a new computational model for space representation called the *isovist field*. The notion of the isovist was first introduced by Benedikt [10] as a tool for modeling human space perception in the context of architectural design. We will discuss why the isovist is also a useful tool for computer space perception.

We will restrict our attention to two-dimensional polygonal spaces. The ideas presented can be generalized to nonpolygonal spaces, as well as to three dimensions. In fact, isovists and isovist fields were motivated in part by Gibson's theory of ecological optics [11], which has itself recently received renewed interest as a

* This research was supported in part by the National Science Foundation under Grant ENG-74-04986.

computational model for vision (see, e.g., Clocksin [12]). In this paper, then, we will be exploring the application of a theory originally designed to account for global aspects of human depth perception mainly to the analysis of two-dimensional shapes. A short discussion of isovists and space perception in relation to architecture is given in Section 3.4.

Let P be a connected subset of the plane. For computational reasons, we will later restrict P to be a polygonal region, possibly with polygonal holes. Let x be a point in P . Then the isovist at point x of P , denoted $V_{x,P}$, or V_x if P is understood, is defined as

$$V_{x,P} = \{y \mid y \in P \text{ and } \mathbf{xy} \cap P = \mathbf{xy}\}.$$

That is, the isovist of point x consists of all points y in P that are *visible* from x .

The notion of an isovist is clearly related to the symmetric axis, or skeleton [13, 14]. The formal distinction is that while the symmetric axis is based on largest circular regions centered at each point and wholly contained in P , the isovist is based on largest star-shaped regions visible from each point that are wholly contained in P . Clearly, the largest circular region of a point is contained in the isovist for that point. The motivational distinction is that the symmetric axis was proposed as a model to help account for biological form and growth, while the isovist was proposed as an explanatory (and a potential computational) model of space perception.

As a simple example of an isovist, consider the polygon P and point x in Fig. 1. V_x is denoted by the hatched area. Note that V_x is a polygon, and that the boundary of V_x can be partitioned into two parts:

- (1) the boundary common with the boundary of P (or boundaries of holes in P)
- (2) the boundary common with the interior of P . This is called the *occluded boundary* of V_x .

Figure 2 is an example of a nonsimple P and V_x for a point x in P . Given a shape, P , and the isovists at all points x in P , we can compute an *isovist field* by assigning to each x in P the value of some feature (such as area) of V_x . Figure 3b contains the *area field* for the shape P in Fig. 3a.

Isovist fields can be used to construct models for human behavior—e.g., one

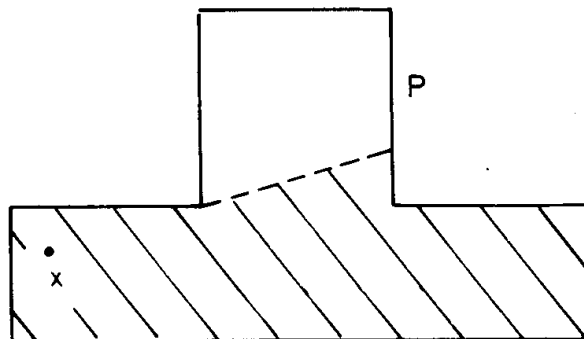
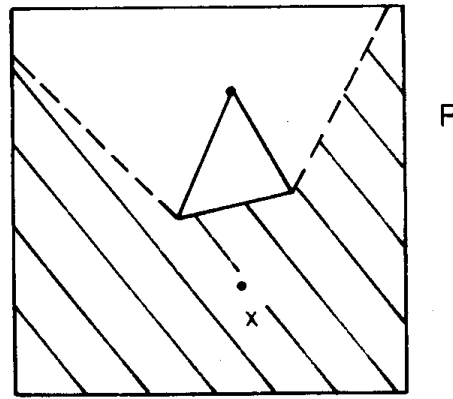


FIG. 1. Polygon P and V_x .

FIG. 2. V_r for nonsimple P .

can test the hypothesis that if a person were asked to hide in a room he would always seek the minimum of the area field. Isoivists and isovist fields can also be used as computational tools for robot plan formation—e.g., compute the shortest traversable path from point a to point b which enables a robot guard to see all points in the room (the shortest path may not be traversable if it involves moving through a narrow gap between two holes). We will examine isovist feature measures and fields later in this paper.

An important notion associated with the isovist is that of a *minimal path* or *minimal set*. We say that the set of points $X = \{x_1, x_2, \dots, x_r\}$ in P is *sufficient* if $P = \cup_{x \in X} V_x$. A set X is *minimal* if X is sufficient, and for all sets Y of points, Y sufficient implies $|X| \leq |Y|$. If we regard X as a sequence, then we can say that X is an ϵ -path if $d(x_i, x_{i+1}) \leq \epsilon$, $1 \leq i \leq r - 1$, where d is some distance measure. If isovists are only computed at a discrete set of grid points in P , and if d is the chessboard distance, then a 1-path is simply an 8-connected path (Rosenfeld and Kak [15]). An ordered set X is a minimal ϵ -path if

- (a) X is an ϵ -path, and
- (b) X is minimal.

Minimal ϵ -paths and minimal sets are of specific interest in both robot planning

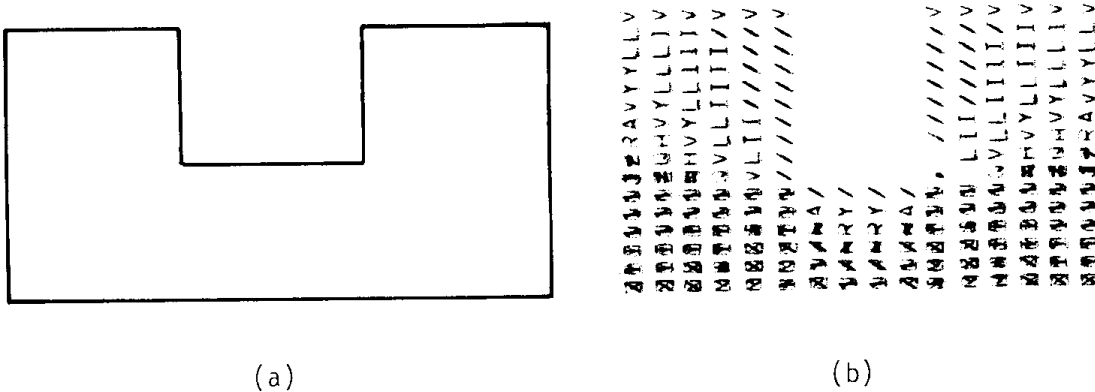


FIG. 3. A U-shape (a) and its area field (b) represented using overstriking. Dark points indicate high area.

and psychological modeling. We might like a robot guard to follow a minimal ϵ -path (ϵ would correspond to the distance the robot would travel before using its vision capabilities to scan the room). Or, if we had to position cameras for the surveillance of a room, we would prefer to put them at points in a minimal set. As a psychological model we might ask if human guards follow minimal ϵ -paths.

An important computational question is how one computes minimal sets and minimal ϵ -paths (or approximations to such sets and paths). We will consider that computation of small sufficient sets in Section 4. We will first discuss the computational considerations involved in forming isovist fields in Sections 2 and 3.

2. COMPUTING THE ISOVIST

In this section we will describe algorithms for computing $V_{x,p}$. We will assume that P is a polygon, although the algorithm can be extended to shapes described by higher-order curves.

We will first assume that P is simply connected; once we can compute $V_{x,p}$ for such P we will describe the extension to multiply connected P 's.

Let P be represented by the sequence of vertices $\{(x_i, y_i)\}_{i=0}^n$. The i th side of the polygon is the line from (x_i, y_i) to (x_{i+1}, y_{i+1}) , subscript addition modulo n .

We say that $v_i = (x_i, y_i)$ is *visible* from x if the line from x to v_i , xv_i , lies entirely within P . Given a suitable representation for P (see Shamos [16]) the question of whether xv_i intersects a side of P (other than one emanating from v_i) can be answered in $O(\log(n))$ time, where n is the number of sides of P .

We first compute the subsequence of vertices of P which are visible from x . We denote this subsequence by $S_x = v_{i_1}, v_{i_2}, \dots, v_{i_m}$. For example, in Fig. 4, $S_x = 0, 1, 2, 5$. If for any $j = 1, \dots, m$, $v_{i_{j+1}} \neq v_{i_j+1} \pmod{n}$, then the pair $v_{i_j}, v_{i_{j+1}}$ is called a *gap*. V_x is completed by filling in the gaps. A gap is filled by constructing the half-lines xv_{i_j} and $xv_{i_{j+1}}$. For each line, we find the closest intersection (to x) of the line with any of the sides $v_{i_j}, \dots, v_{(i_{j+1}-1)}$ (it may be that no such intersection exists). Call these intersections $g_{i_j}, g_{i_{j+1}}$ (see Fig. 5).

We can merge S_x and the gap fillers to finally compute V_x . Any side in V_x connecting a vertex from P and a gap filler is called an *occluded side*. Occluded sides are sides of V_x which are not coincident with sides of P .

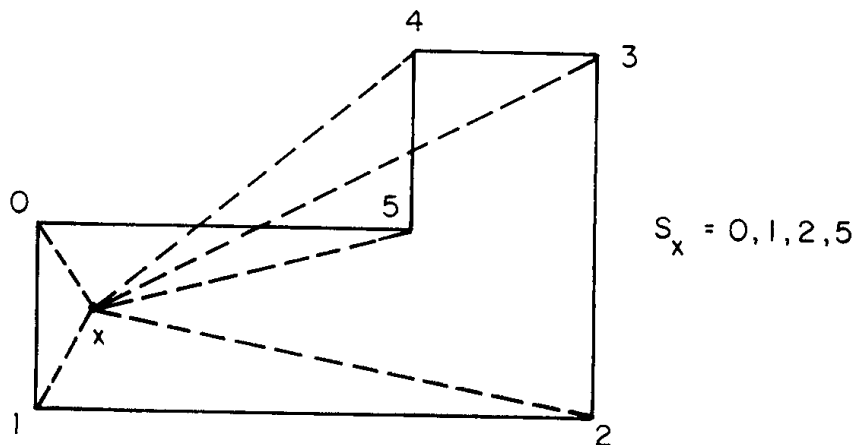


FIG. 4. Visible vertices at x .

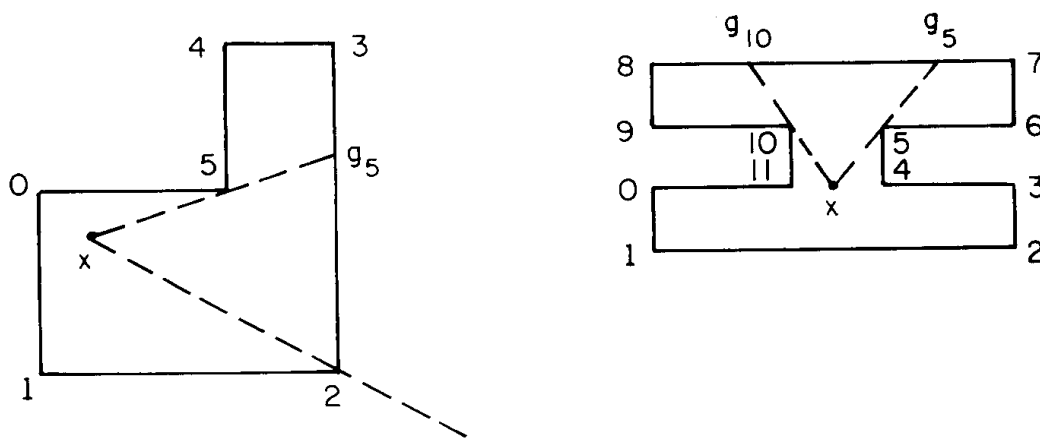


FIG. 5. Computing gap fillers.

In what follows, we will consider the effects of introducing *barriers* and *holes* into P .

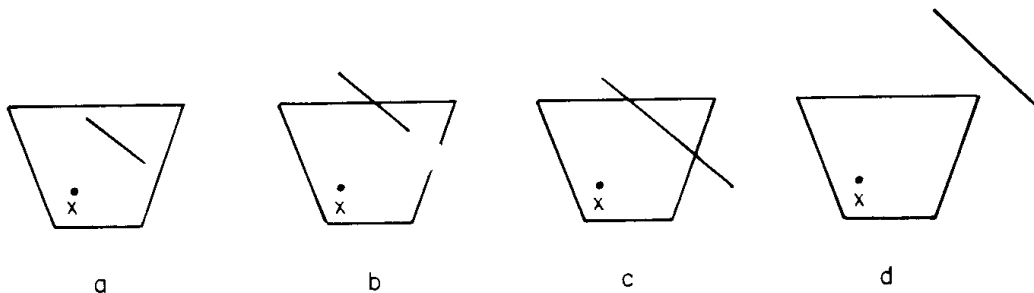
A *barrier* in P is a straight-line segment wholly contained in P . Let x be a point in P and let V_x be the isovist at x . Let b be a barrier in P . Then there are four relations that b might bear to V_x :

- (1) Both endpoints of b may be in V_x (see Fig. 6a),
- (2) One endpoint of b may be in V_x (see Fig. 6b),
- (3) b may pass through V_x (see Fig. 6c),
- (4) b may be disjoint from V_x (see Fig. 6d).

Let V'_x be the new isovist at x resulting from the introduction of b . Note that if the left end of b (when viewed from x) is outside V_x , then odd-numbered intersections of b with V_x signal entrances of b into V_x and even-numbered intersections signal exits. Vertices of V_x between entrances and exits are *excluded* from V'_x . Vertices of V_x between exits and entrances are *included* in V'_x . If the left end of b is inside V_x , then odd-numbered intersections of b with V_x signal exits and even-numbered ones signal entrances.

A *hole* (or a solid obstruction) is a polygon P' wholly contained in P . To compute V'_x given the introduction of a hole in P we:

- (1) check to see if $x \in P'$. If so, we define $V'_x = \phi$, since x is no longer in P .
- (2) Otherwise treat each side of the hole as a barrier.

FIG. 6. Types of barriers in P .

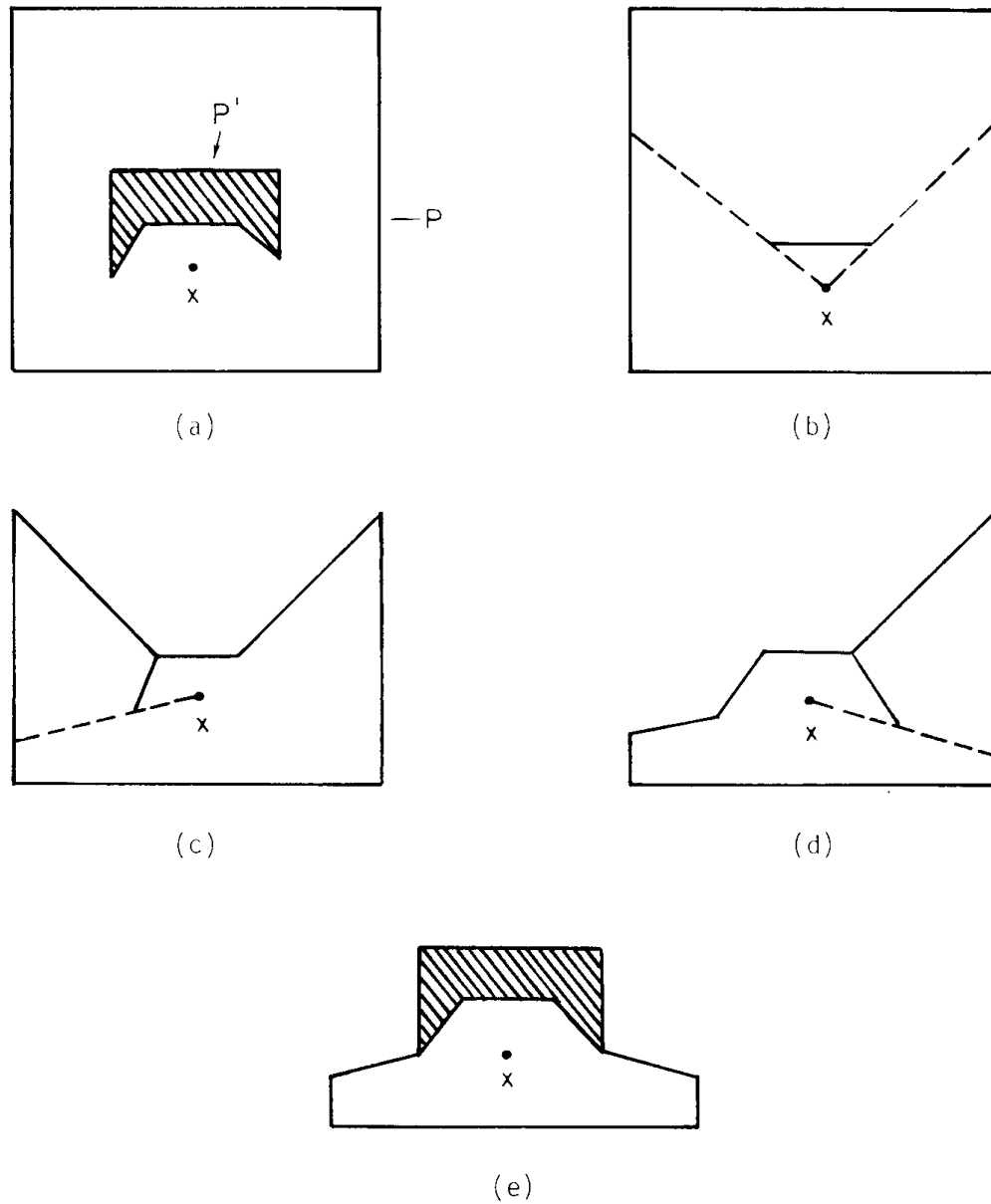


FIG. 7. Introducing a hole in P .

Figure 7 shows the results of successively treating each side of a hole, P' , as a barrier to compute the isovist at point x in P after the introduction of P' . Note that we considered the sides of P' in increasing order of their distance from x . In this way, the last three sides of P' resulted in no changes to V_x .

An important extension of the notion of a hole is the notion of *horizon*. The computation of V_x assumes that the visibility from any point is potentially infinite; the presence of the border (of P) and barriers is what makes V_x finite. There is no prior bound on the radius of V_x .

The notion of a horizon is intended to model the limited view of a human perceiver (the limitation derives more from psychological constraints than from physical constraints). The horizon is, ideally, a circle of radius r centered at x .

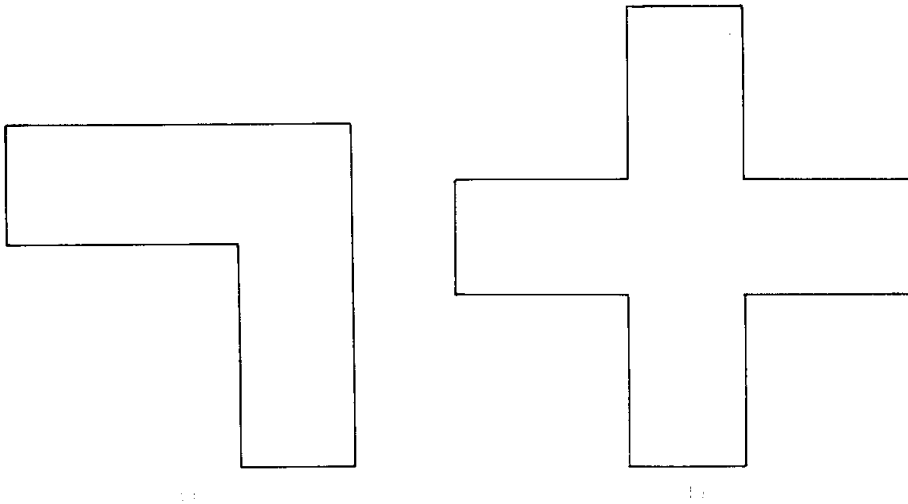


FIG. 8. Two simple shapes.

For ease of computation, we might model the horizon as a diamond or an octagon of radius r centered at x . We call this the *horizon shape*, H . (Note: Diamonds and octagons are the most compact digital shapes; see Rosenfeld [17].) The *horizon-limited isovist* at x , V_x^r , is the intersection of V_x with the horizon shape centered at x . V_x^r can be computed by a procedure identical to that for dealing with a hole except for the exclusion of the test for membership of x in P' . We will not specifically discuss the computation of isovist fields for horizon-limited isovists in this paper.

3. ISOVIST FIELDS

In this section we will discuss the computation of isovist fields and display some of these fields. We will discuss both the computational aspects of computing the isovist fields, and the applications of the fields to robot planning, psychological modeling and architectural design (Section 3.4).

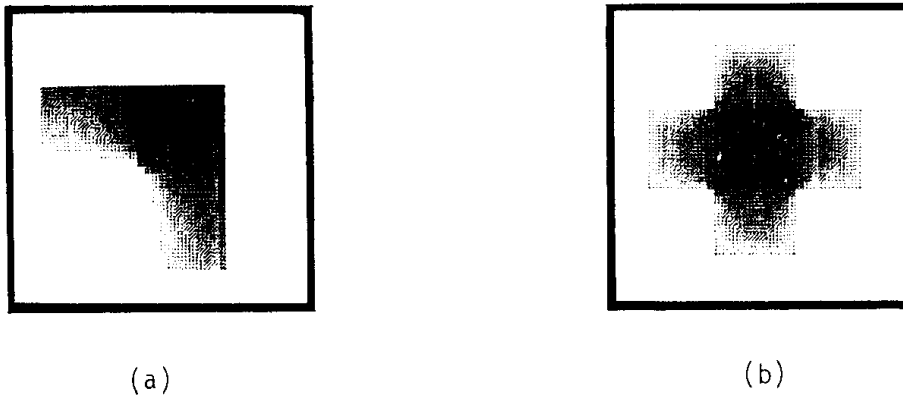


FIG. 9. Area fields.

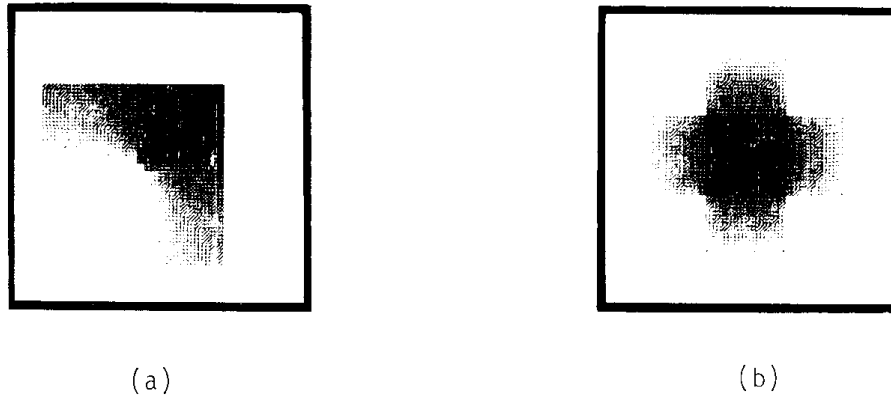


FIG. 10. Perimeter fields.

3.1. The Area Isovist Field— \mathcal{A}

Suppose that the vertices of V_x are $\{v_i = (x_i, y_i)\}_{i=0}^n$. Then the area of V_x , A_x , is

$$A_x = \sum_{i=0}^n x_i(y_{i+1} - y_{i-1}).$$

Figure 8 shows two simple shapes. Figure 9 shows the isovist area field, \mathcal{A} , for the shapes in Fig. 8.

3.2. The Perimeter Field— \mathcal{B}

The length of the boundary of V_x , the perimeter of V_x , B_x , is

$$B_x = \sum_{i=0}^n d(v_i, v_{i+1}).$$

Figure 10 shows the perimeter fields for the shapes in Fig. 8.

It is obvious that if P is convex, then \mathcal{B} is constant. However, \mathcal{B} constant does not imply P convex. Consider two tangent, closed circular sets, for example. For such a set, \mathcal{B} is constant.

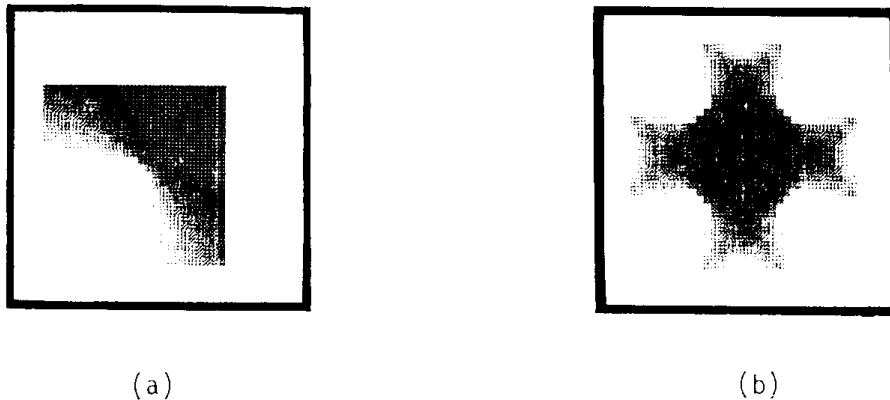


FIG. 11. Compactness fields.

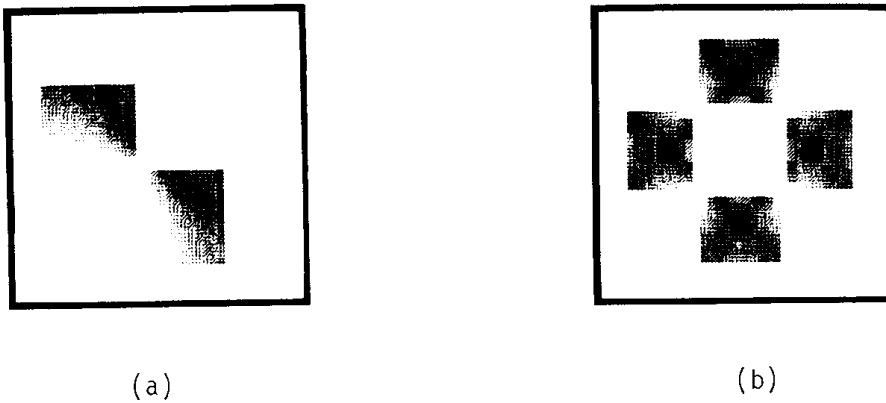


FIG. 12. Occlusivity fields.

An interesting field which can be derived easily from \mathcal{G} and \mathcal{B} is the *compactness field*, \mathcal{C} , defined at point x as $C_x \equiv B_x^2/A_x$. This, of course, is also constant for a convex P (but again, constant \mathcal{C} does not imply P convex). Figure 11 contains the compactness fields for the forms in Fig. 8.

Another useful field related to the perimeter field is the *occlusivity field*. Recall that in the computation of V_x the occlusivity of V_x , O_x (with field \emptyset), is the total length of the occluded sides of V_x (see Section 2). We can then also define the visible perimeter field, $\mathcal{V}\mathcal{P}$, as $\mathcal{P}-\emptyset$. Figures 12 and 13 contain \emptyset and $\mathcal{V}\mathcal{P}$ for the shapes in Fig. 8.

The area and visible perimeter fields could serve an important function in robot plan formation. A reasonable constraint to place on a path which a robot might traverse in surveying some environment is that if the robot moves along the digital path $\{x_1, x_2, \dots, x_n\}$, then the isovists at consecutive points, V_{x_i} and $V_{x_{i+1}}$, share a sufficiently high percentage of area. In this way, the robot could use his perception of V_{x_i} to guide his perception of $V_{x_{i+1}}$. If $V_{x_i} \cap V_{x_{i+1}}$ were small, then no such expectations would be available for facilitating the processing of $V_{x_{i+1}}$. A similar argument could be made concerning the visible perimeter since most of what the robot must perceive is contained in the visible surfaces surrounding him.

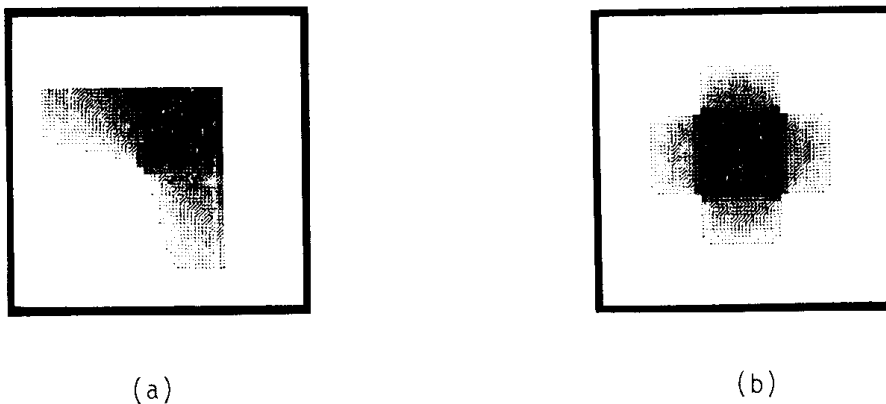


FIG. 13. Visible perimeter fields.

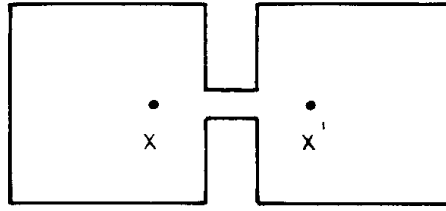


FIG. 14. $|A_x - A_{x'}|$ small but $V_x \cap V_{x'}$ small also.

A reasonable heuristic to bring to bear on choosing a path, then, is that the maximal rate of change of area (or visible perimeter) along that path is bounded, i.e.,

$$|A_{x_i} - A_{x_{i+1}}| < b.$$

(Note that $|A_{x_i} - A_{x_{i+1}}| < b$ does not imply that V_{x_i} and $V_{x_{i+1}}$ share much common area, since they might, e.g., be on opposite sides of a symmetric “pinched” space, such as the one shown in Fig. 14. The safer strategy, then, is to compute $A(V_{x_i} \cap V_{x_{i+1}})$.)

Another possible point of view is that since computer vision is expensive even when given a powerful set of expectations, we should compute a small, sufficient set (cf. Section 4). Thus, we would minimize the number of times that the robot would have to invoke his visual capabilities. Section 4 discusses the computation of small, sufficient sets.

Note, also that the Θ field (and the $\cup\mathcal{P}$ field) decompose the cross into simple pieces corresponding to the “lobes” of the cross and the center of the cross. This suggests that fields such as Θ should be useful tools for shape decomposition. In fact, necks in shapes are places where fields such as Θ and \mathcal{B} are changing rapidly. The problem of shape decomposition based on isovist fields will be treated in a subsequent paper. Note that the shape decomposition scheme proposed by

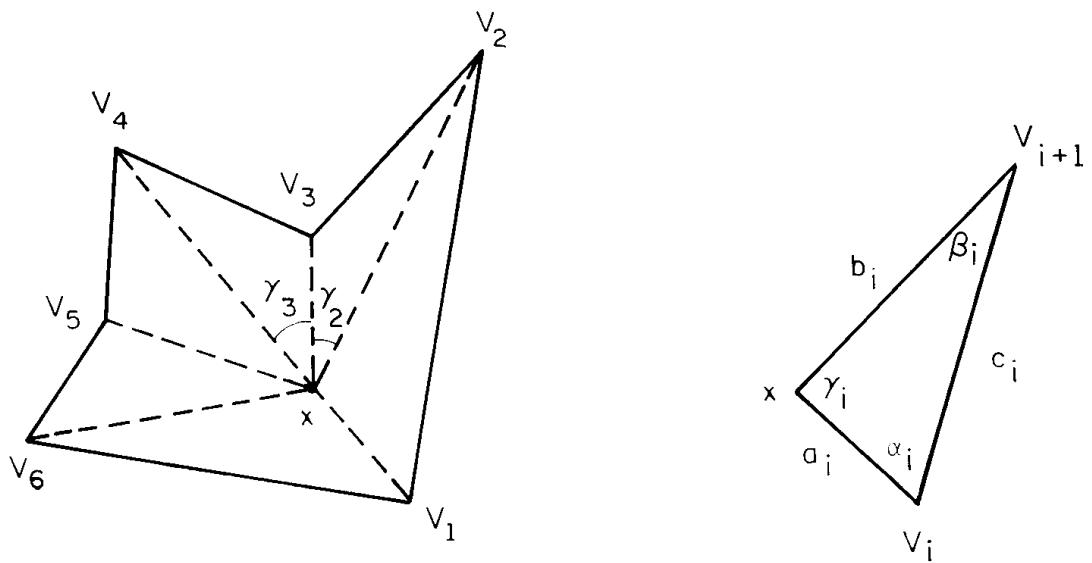
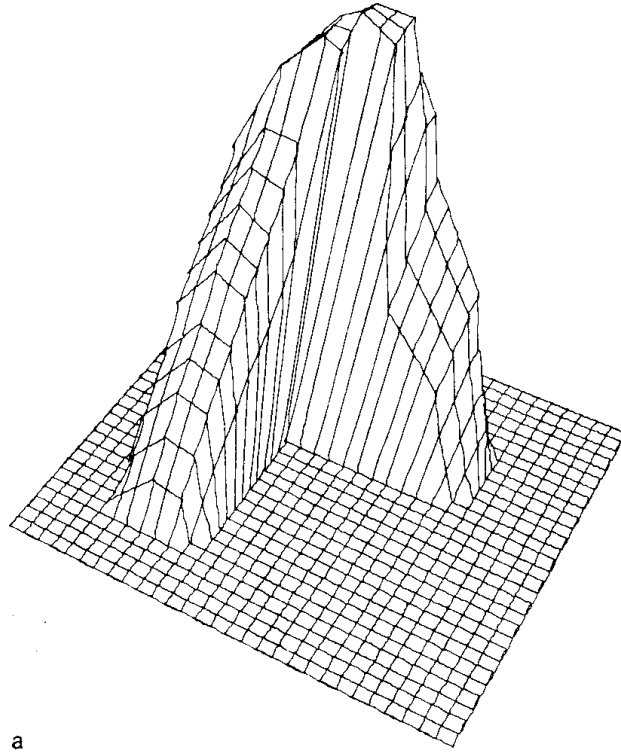


FIG. 15. Computing moments.



a

FIG. 16a. M_1 field, \mathfrak{M}_1 , for Fig. 8a (perspective plot).

Haralick and Shapiro [18], which starts by computing all pairs of perimeter points p and p' such that $p \in V_{p'}$ was implicitly using ideas related to isovists.

3.3. Radial Moment Fields

Since V_x is star-shaped from x , an equivalent way of representing V_x is in polar form $d = r(\theta)$, where $r(\theta)$ is the length of the line from x to the boundary of V_x in direction θ .

The p th moment of V_x is then

$$M_p = \frac{1}{2\pi} \int_0^{2\pi} (r(\theta) - \bar{r}(\theta))^p d\theta,$$

where

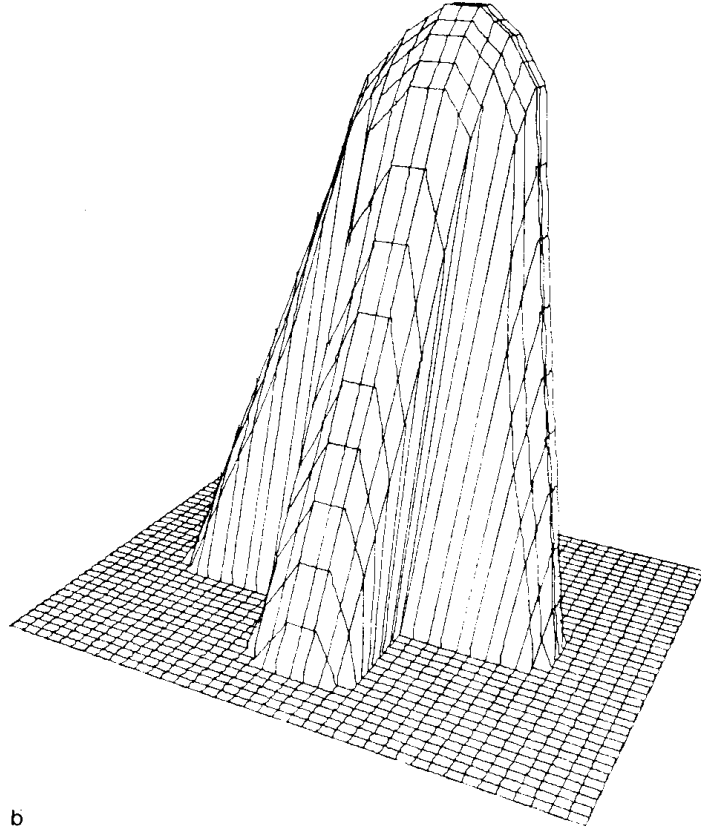
$$\bar{r}(\theta) = \frac{1}{2\pi} \int_0^{2\pi} r(\theta) d\theta.$$

In the special case where V_x is a polygon, it can be shown that

$$\begin{aligned} M_1 &= a_1, \\ M_2 &= a_2 - M_1^2, \\ M_3 &= a_3 - 3M_1 a_2 + 2M_1^3, \end{aligned}$$

where

$$a_p = \sum_{i=1}^n \frac{\gamma_i}{2\pi} a_p(i)$$

FIG. 16b. M_1 field, \mathfrak{M}_1 , for Fig. 8b.

and

$$a_1(i) = \frac{a_i b_i \sin \gamma_i}{c_i \gamma_i} \log \left| \frac{(c_i + a_i - b \cos \gamma_i)(c_i + b_i - a_i \cos \gamma_i)}{a_i b_i \sin^2 \gamma_i} \right|,$$

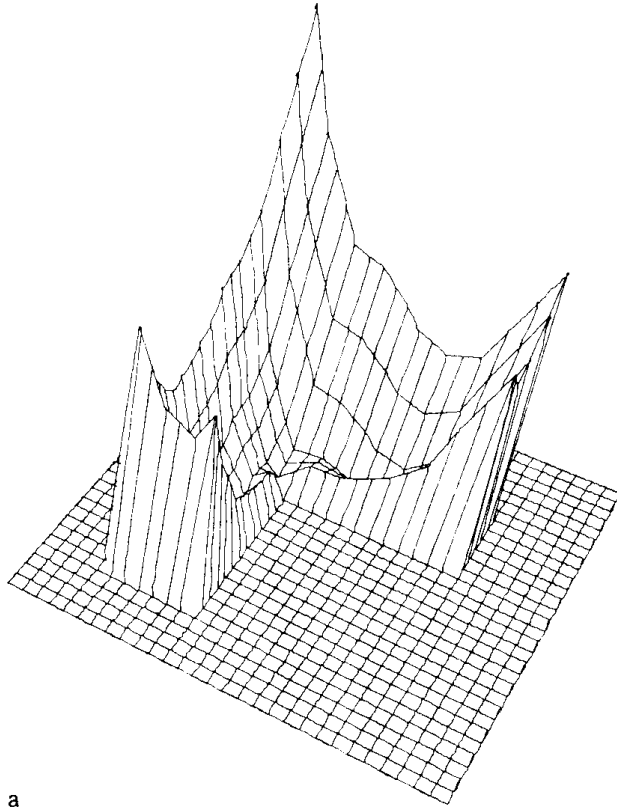
$$a_2(i) = \frac{1}{\gamma_i} \left(\frac{a_i b_i}{c_i} \sin \gamma_i \right)^2 (\cot \alpha_i + \cot \beta_i),$$

$$a_3(i) = \frac{1}{2\gamma_i} \left(\frac{a_i b_i}{c_i} \sin \gamma_i \right)^3 [\operatorname{cosec} \alpha_i \cot \alpha_i + \operatorname{cosec} \beta_i \cot \beta_i \\ + \log |[(\operatorname{cosec} \alpha_i + \cot \alpha_i)(\operatorname{cosec} \beta_i + \cot \beta_i)]|]$$

(see Fig. 15 for the definitions of α_i , β_i , γ_i , a_i , b_i , c_i).¹

Figures 16–18 contain the moment fields (\mathfrak{M}_1 , \mathfrak{M}_2 , \mathfrak{M}_3) for the shapes in Fig. 8. In the context of isovists, \mathfrak{M}_1 represents the deviation from the mean of the perimeter's distance to x , \mathfrak{M}_2 the variance, and \mathfrak{M}_3 the skewness of the perimeter distribution relative to x .

¹ We are grateful to Professor Frederic Ancel of the Mathematics Department of the University of Texas at Austin for providing the geometrical constructions and derivations which led to these formulas.



a

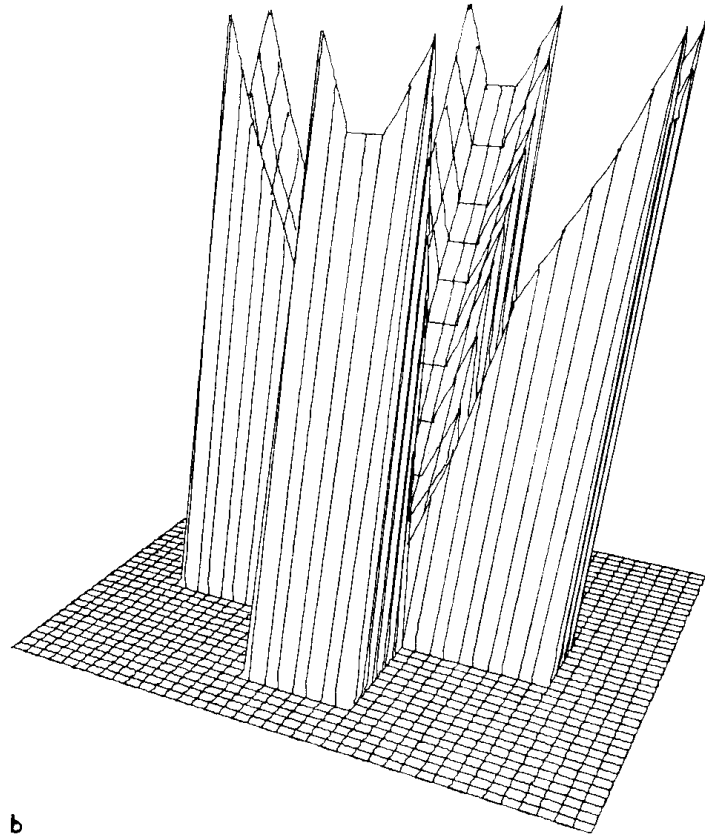
FIG. 17a. M_2 field, \mathfrak{M}_2 , for Fig. 8a.

3.4. Psychological Relevance of Isovist Fields and Some Possible Applications

In the previous subsections we have introduced a variety of isovist fields and discussed their relevance to computer space perception. In this subsection, we would like to elucidate some of the psychological and architectural significance of these fields.

As a first example, a number of authors have recently come to view the problem of *privacy* as one of regulation of personal information, that is, as the achieving of “an optimum balance . . . between the ‘information’ which comes to a person and that which he puts out” (Canter and Kenny [19]; cf. also Altman [20]). When we consider sources of (visual) information to be distributed in some definite way in space, then each isovist “covers” a definite subset of those sources. The isovist size measures, such as area and perimeter, approximate the (potential) amount of information available at x as well as the (potential) “audience size” or exposure of a person at x . Therefore one would expect that privacy-related path and location choice (and the definition of “public” and “private spaces” in general) will pay, at least unconsciously, much attention to the maxima, minima, and gradients of fields such as the area and perimeter fields.

There are situations and environments in which one typically wishes to see much without being overly exposed on all sides. Here area alone will not suffice and it is better to consider, too, the skewness (\mathfrak{M}_3) of the distribution $r(\theta)$. It

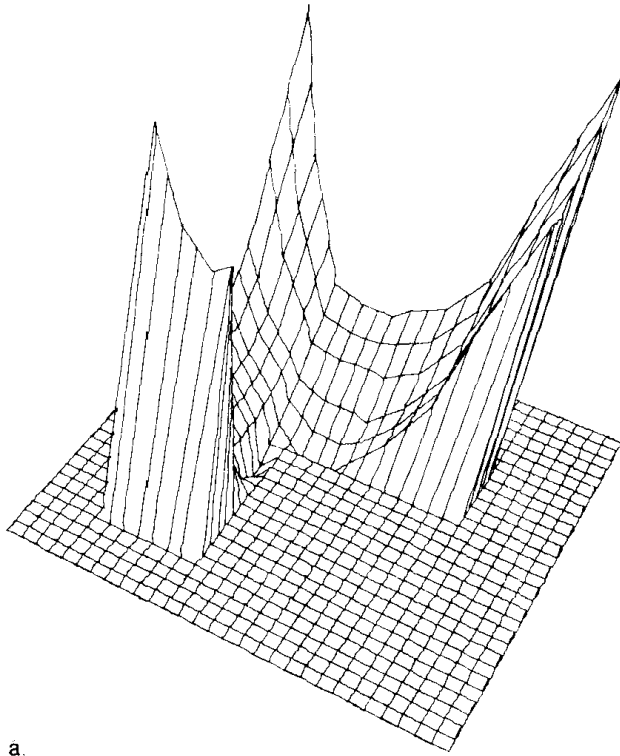


b

FIG. 17b. M_2 field, \mathfrak{M}_2 , for Fig. 8b.

measures the extent to which radials are concentrated in a certain angular region and tends to be large close to surfaces and in corners (although high \mathfrak{M}_3 does not invariably entail this condition: further conditions are also relevant). In a given environment, points in space characterized by high area and \mathfrak{M}_3 thus tend to fulfill our conditions for good view and low angular exposure. It is a matter for further research whether such commonly observed behaviors as preferring a table with a view in a corner or a table against a wall or pillar in a restaurant (or institutional dayroom; Sommer [21]), or waiting in railway stations close to pillars in areas of good visibility (Canter [19, p. 133]), are amenable to analysis and prediction based on isovist field analysis.

Consider another related example. Newman [22, pp. 30–34], reporting on the incidence of crime in and around urban residential buildings, pointed out the significant relationship of visibility to crime incidence. The intending criminal is interested in three things with respect to spatial characteristics of the environment: (1) being inconspicuous, (2) being safe from sudden detection, and (3) having an avenue for escape. The first two factors are describable in good part as attributes of the isovist, area and oclusivity, respectively. The hypothesis that crime such as vandalism, burglary, or assault will tend to occur in regions of coincident local minima in area and oclusivity seems to be borne out in Newman's data. He reports a high incidence of crime in elevators, certain lobbies, and corridor



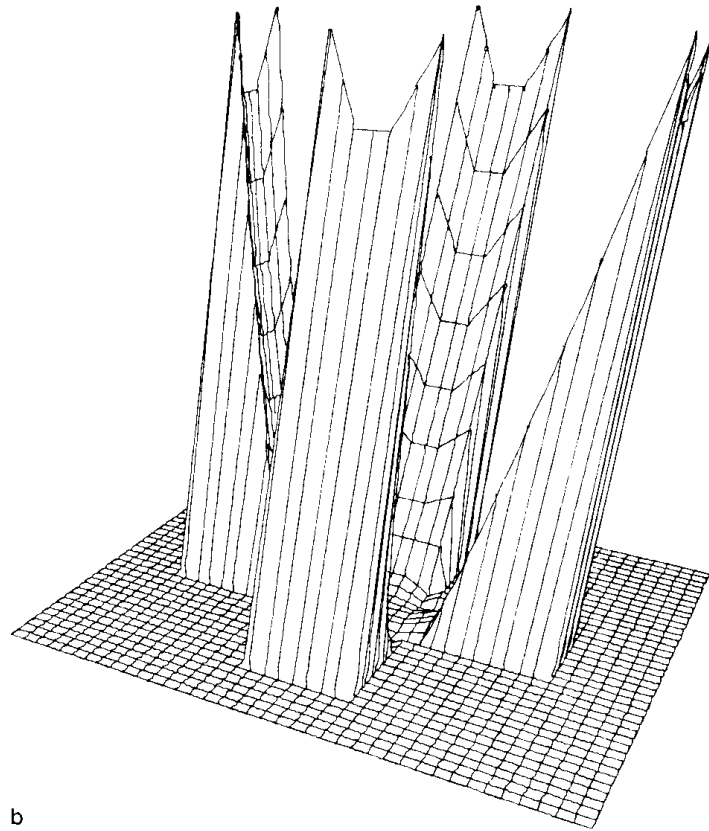
a.

FIG. 18a. M_3 field, \mathfrak{N}_3 , for Fig. 8a.

types. But for less intuitively obvious cases, only more detailed data about the spatial location of incidents of crime will serve to confirm or reject this hypothesis. If confirmed, computer generation of the area and oclusivity fields of a proposed building or group of buildings might well help to predict likely trouble spots and be a guide in redesign. (We do not mean to imply, of course, that visibility criteria are the sole or most salient determinants of crime in a “defensible space” theory (cf. Mawby [23]).) Optimal surveillance paths, of course, may correspond to minimal sufficient paths as already defined.

Many writers have remarked qualitatively about the need or desirability for spatial diversity in the environment (e.g., Rapaport and Hawkes [24]). From open to closed areas, field to forest, peak to valley, plaza to vestibule, courtyard to street, and so on, the opportunity exists to typify and quantify “types of space” and the transitions between them in a new way since each has characteristic isovists and isovist fields (see also Thiel [25]). In urban and regional studies, straightforward use of the isovist (or “viewshed”) can already be found (cf. Lynch [26, pp. 98–100, 138–142]).

It is also conceivable that terms such as “hall,” “street,” “court,” “colonnade” . . . might in good part be *definable* in terms of the kinds of isovists and isovist fields they generate. If this were possible partially or within limits, as should often be true, a direction seems clear: to design environments not by initial specification of walls, surfaces, and openings, but by specification of the desired (potential) experience-in-space, that is, by designing fields directly; compare Thiel’s [25] “envirotecture” (see also Sommer [27, p. 132]). Be that



b

FIG. 18b. M_3 field, \mathfrak{N}_3 , for Fig. 8b.

as it may, it seems clear that feature measures describing the shape and size of isovists can create a group of scalar fields unique to a given environment. These fields in turn characterize the environment and appear to be correlated with certain human spatial perceptions and behaviors. An experimental program now under way is an application and test of some of the hypotheses. The problem chosen is that of the perception of "spaciousness"; of how large or small an environment appears because of its shape and/or the observer's position and path of movement. Two series of experiments are entailed, preceded by an analysis of the statistical behavior of isovist measures relative to each other, with and without "architectural constraint." The first series employs models, the second full-size experimental environments. In both, the perception of spaciousness is tested against systematic variation of isovist measures in architectural environments of objectively equal size (area/volume).

In the realm of computer vision, parallels to the above observations apply. Work, to be reported in a subsequent paper, indicates that medial axis transforms and shape decomposition can be effected from isovist fields. Isovist fields, like fingerprints, may also be useful in typifying dissimilar or identifying and distinguishing otherwise similar shapes. Analysis of depth information output from range-finding devices may also be fruitful: we have already remarked about the problems facing a (robot) guard. Indeed, research in strategic search and sur-

veillance (e.g., Gallagher's discussion of "intervisibility" [28]) could well benefit from the computation of sufficient sets and paths from local information, and an investigation of various "hide and seek" algorithms.

4. SUFFICIENT SETS OF ISOVISTS

In this section we will investigate the relationship between sufficient sets (i.e., sets of points whose isovists cover the original shape) and the skeleton of the shape. As before, we are restricting our attention to shapes with polygonal borders.

It is interesting that we can distinguish between notions of *area sufficiency* and *perimeter sufficiency*. We have, up to now, only considered area sufficiency—i.e., a subset B of P is *area sufficient*, a -sufficient, if $\cup_{b \in B} V_b = P$. If we let \bar{P} denote the perimeter of P , then we can say that a set B is *perimeter sufficient*, p -sufficient, if $\cup_{b \in B} \bar{V}_b = \bar{P}$. Clearly, B a -sufficient implies B p -sufficient. However, the converse does not hold. Consider Fig. 19. The set $B = \{b_1, b_2, b_3\}$ is p -sufficient, but not a -sufficient.

In what follows, we will restrict our attention to a -sufficiency, so that "sufficiency" will mean a -sufficiency. It is, of course, obvious that the skeleton itself is a sufficient set, since the largest disk D_x , centered at a point x in P which is wholly contained in P is clearly contained in the isovist at x , V_x ; i.e., $D_x \subseteq V_x$. However, the skeleton has "too many" points to be of interest. We will show that the set of *skeleton branch points*, i.e., the endpoints of skeleton branches, constitutes a sufficient set.

Montanari [29] proves that there are only three types of branches in the

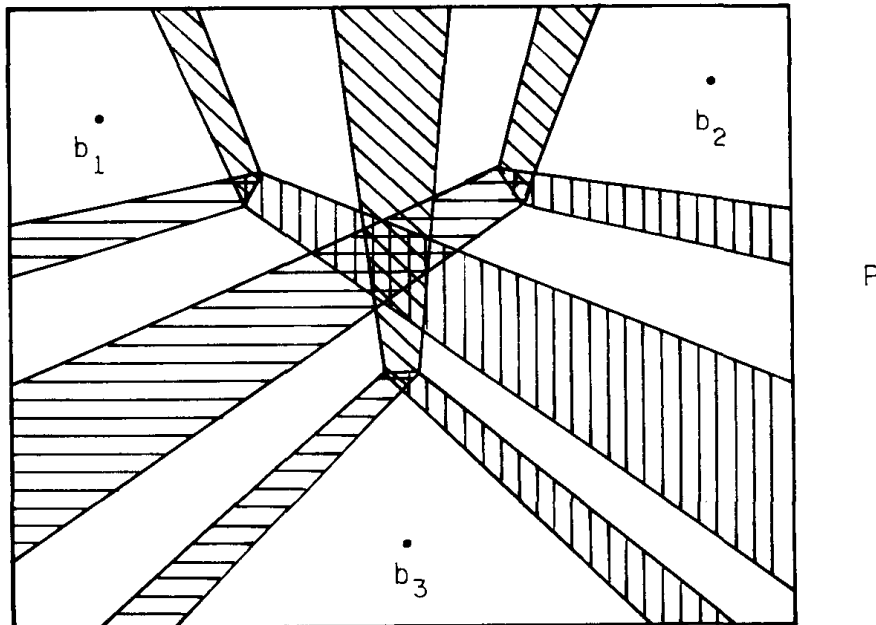


FIG. 19. $\bar{V}_{b_1} \cup \bar{V}_{b_2} \cup \bar{V}_{b_3} = \bar{P}$. Area marked with $|$ is $P - V_{b_1}$; $—$ is $P - V_{b_2}$; and \backslash is $P - V_{b_3}$. Note that all of the border of P is contained in some isovist, but the crosshatched area in the center of P is not.

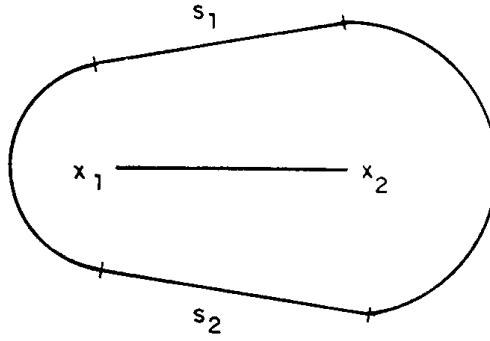


FIG. 20. For a type 1 branch, $D_{x_1 x_2}$ is convex.

skeleton of a polygon :

(1) A straight-line segment generated by wavefronts propagating from two sides of the polygon. We will call such a branch a *type 1 branch*.

(2) A straight-line segment formed by the circular wavefronts propagating from two concave angles of the polygon. We will call such a branch a *type 2 branch*.

(3) A parabolic arc formed by a circular wavefront and a straight wavefront. The concave angle causing the circular wavefront is the focus of the parabola, while the straight side causing the straight wavefront is the directrix. We will call such a branch a *type 3 branch*.

LEMMA. Let $x_1 x_2$ be a branch of the skeleton of a polygon P . Let $D_{x_1 x_2} = \bigcup_{x \in x_1 x_2} D_x$. Then if p is a point in $D_{x_1 x_2}$, then either $\mathbf{x}_1 p \subseteq D_{x_1 x_2}$ or $\mathbf{x}_2 p \subseteq D_{x_1 x_2}$. Equivalently, if x is a point on $x_1 x_2$, then $D_x \in (V_{x_1} \cup V_{x_2})$.

Proof. By cases.

(1) Suppose $x_1 x_2$ is a type 1 branch. Then $D_{x_1 x_2}$ is shaped as shown in Fig. 20, since the propagation velocity along the branch is constant. Here, s_1 and s_2 are the sides of P giving rise to the branch $x_1 x_2$. Since, in this case, $D_{x_1 x_2}$ is convex, it is star-shaped from both x_1 and x_2 .

(2) Suppose $x_1 x_2$ is a type 2 branch. Then we can show that $D_{x_1 x_2} = D_{x_1} \cup D_{x_2}$. To see this, consider Fig. 21. Consider D_{x_3} and a clockwise traversal of its border, \bar{D}_{x_3} . The borders of all the disks on $x_1 x_2$ intersect at the same two points, p_1 and p_2 . The intersection of \bar{D}_{x_3} with \bar{D}_{x_2} at p_2 marks the departure of \bar{D}_{x_3} from D_{x_2} , since $y \in D_{x_2}$ and the intersection of \bar{D}_{x_3} with \bar{D}_{x_2} at p_1 marks the entrance of \bar{D}_{x_2} into D_{x_2} . Therefore, the only part of \bar{D}_{x_3} not contained in D_{x_2} is the arc between p_2 and p_1 . But, by similar reasoning, the intersection of \bar{D}_{x_3} with \bar{D}_{x_1} at p_1 is the departure of \bar{D}_{x_3} from D_{x_1} (since $y \notin D_{x_1}$) and the intersection of p_2 is the entrance. But then $\bar{D}_{x_3} \subseteq D_{x_1} \cup D_{x_2}$, and since D_{x_3} is convex, $D_{x_3} \subseteq D_{x_1} \cup D_{x_2}$. So

$$\bigcup_{x \in x_1 x_2} D_x = D_{x_1} \cup D_{x_2} \cup \left[\bigcup_{x_3 \in x_1 x_2} D_{x_3} \right] = D_{x_1} \cup D_{x_2}, \quad \text{s.t. } x_3 \neq x_1, x_3 \neq x_2.$$

(3) Suppose $x_1 x_2$ is a type 3 branch. Then we can show (see Fig. 22) that $D_{x_1 x_2} = D_{x_1} \cup D_{x_2} \cup X$, and that all points in $D_{x_1 x_2}$ are visible from either x_1 or x_2 . First, it is clear that the line segment from $(a, 0)$ to $(c, 0)$ forms part of $\bar{D}_{x_1 x_2}$. Now, for any x_3 on $x_1 x_2$, \bar{D}_{x_3} intersects both \bar{D}_{x_1} and \bar{D}_{x_2} at the focus. Furthermore,

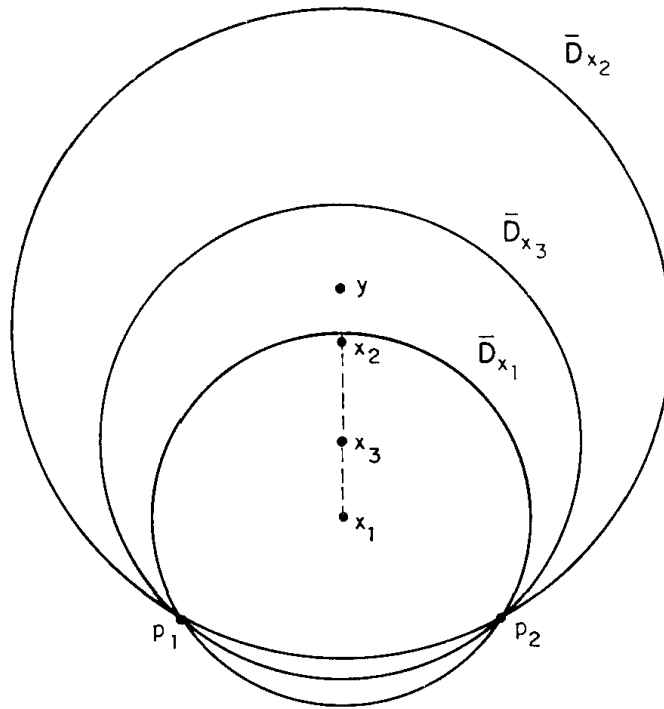


FIG. 21. For a type 2 branch, $D_{x_3} \subseteq D_{x_1} \cup D_{x_2}$, $x_3 \in x_1x_2$.

\bar{D}_{x_3} intersects \bar{D}_{x_1} at a point to the right of $(a, 0)$ and intersects \bar{D}_{x_2} at a point to the left of $(c, 0)$. The only points in D_{x_3} that are not in $D_{x_1} \cup D_{x_2}$ are those in $D_{x_3} \cap X$. We will show that all points in $D_{x_3} \cap X$ are visible from x_1 (they are also visible from x_2). Suppose not. Then there is a $p \in D_{x_3} \cap X$ such that $\mathbf{x}_1\mathbf{p} \not\subseteq P$. Let p' be the first point on the vector $\mathbf{x}_1\mathbf{p}$ such that $p' \in P$ (one must exist since otherwise $\mathbf{x}_1\mathbf{p} \subseteq P$). Since $D_{x_1} \subseteq P$, it must be that $p' \in X$. Let p' have coordinates (g, h) . Then clearly $a < g < c$. Let $x_4 = (j, h)$ be the intersection of the line $y = h$ with the parabola. Then $p' \in D_{x_4} \subseteq P$. But then $p' \in P$, contradicting the assumption that $p' \notin P$. Therefore, every point p in X is visible from x_1 . Since $D_{x_1} \subseteq V_{x_1}$ and $D_{x_2} \subseteq V_{x_2}$ and we have shown $X \subseteq V_{x_1}$, $D_{x_1x_2} \subseteq V_{x_1} \cup V_{x_2}$. //

Using this lemma, we can prove the following theorem.

THEOREM. Let $B = \{b_1, \dots, b_n\}$ be the branch points of the skeleton of P . Then $P = \bigcup_{b \in B} V_b$.

Proof. Clearly $\bigcup_{b \in B} V_b \subseteq P$. Let $p \in P$. Then for some x on the skeleton of P , $p \in D_x$. Let x_1x_2 be the branch containing x . Then, since by the lemma, $D_x \subseteq V_{x_1} \cup V_{x_2}$, it must be that $x \in V_{x_1} \cup V_{x_2} \subseteq \bigcup_{b \in B} V_b$. But then $P \subseteq \bigcup_{b \in B} V_b$. //

Now, the set B is obviously not minimal; for a rectangle, e.g., B contains two points, whereas only one point is required for the minimal set of any convex shape. In fact, although the skeleton branch points constitute a convenient (to compute) central set of points from which to construct a small sufficient set (see below), it is unfortunately *not* the case that the smallest subset of the set of branch points that is sufficient is also minimal.

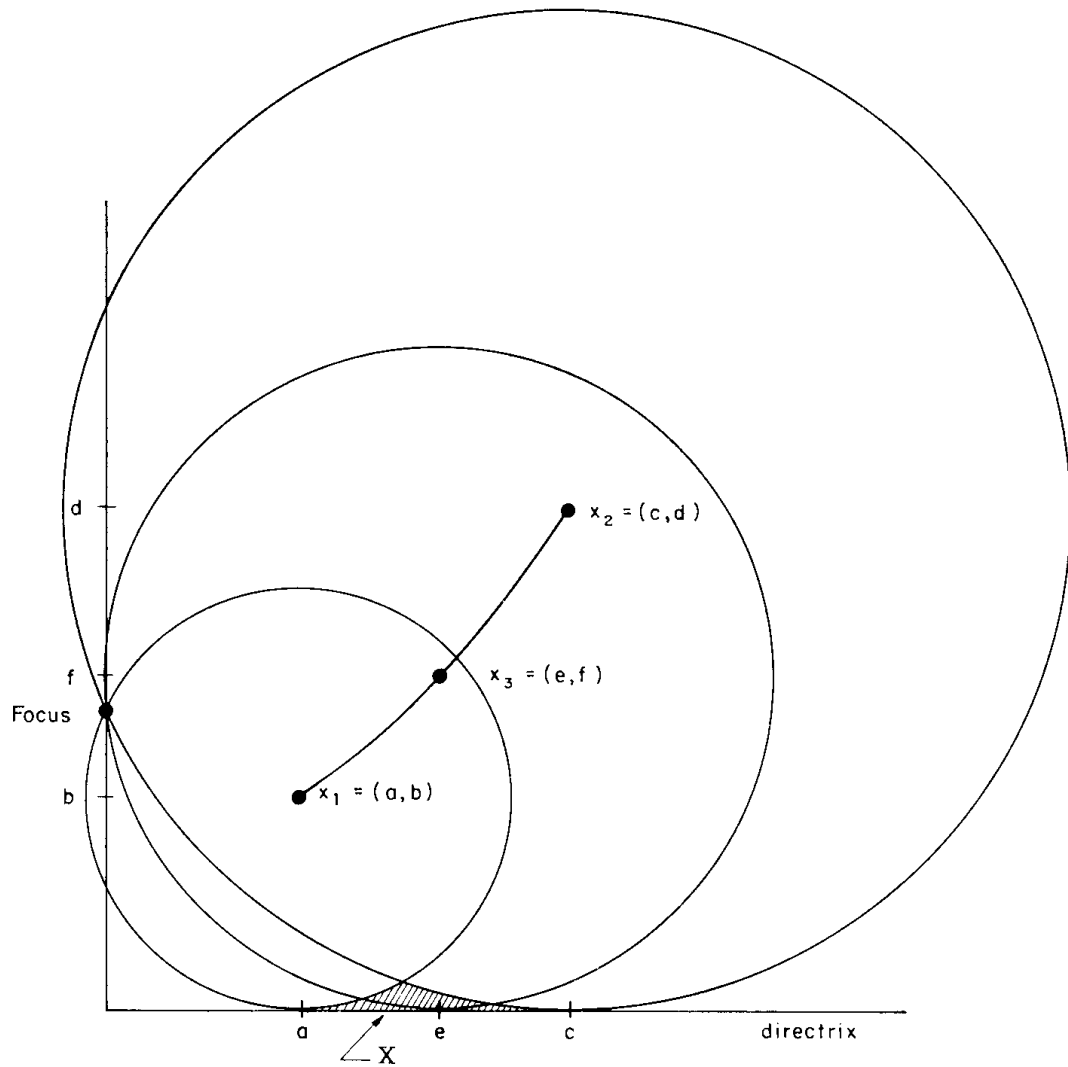


FIG. 22. D_{x_1, x_2} for a type 3 branch.

Fact. The skeleton of a star-shaped polygon does *not* necessarily pass through the kernel.

Consider Fig. 23. The kernel is the crosshatched region X . The skeleton of this figure will not pass through area X . Therefore, the smallest sufficient subset of the skeleton branch points will have size at least 2. Of course, discovering that a figure is star-shaped is computationally simple (see Shamos [16]); however, one can imagine a regular duplication of such figures. Here, the size of a minimal sufficient set is a number unobtainable using the skeleton-based approach.

We can, however, establish an easily obtained lower bound. Let F be a minimal sufficient set for P and let $|F|$ denote the size of F .

PROPOSITION 1. *Let P be a polygon with vertices $\mathcal{P} = \{p_1, \dots, p_n\}$ and isovists at those vertices V_{p_1}, \dots, V_{p_n} . Let \mathcal{P}' be the largest subset of \mathcal{P} with the property that if $p_i, p_j \in \mathcal{P}'$, $i \neq j$, then $V_{p_i} \cap V_{p_j} = \emptyset$. Then $|F| \geq |\mathcal{P}'|$.*

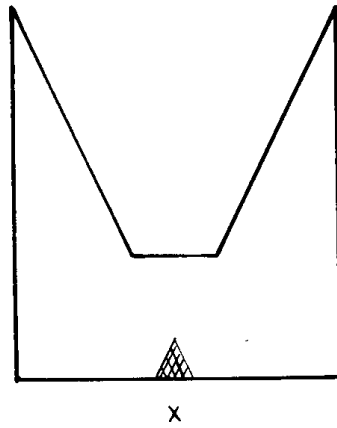


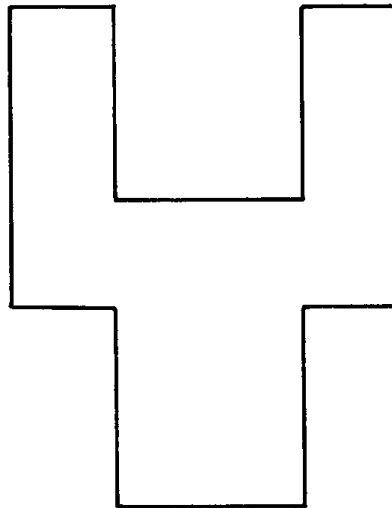
FIG. 23. Skeleton does not pass through kernel.

Proof. Suppose $|F| < |\mathcal{O}'|$. Let $X = \{x_1, \dots, x_{|\mathcal{O}'|-1}\}$ be a sufficient set. Then since $|X| < |\mathcal{O}'|$, there must be an $x_i \in X$ such that for some pair $p_j, p_k \in \mathcal{O}'$, x_i must see both p_j and p_k . But then $V_{p_j} \cap V_{p_k} \neq \emptyset$ since x_i is in the intersection. Thus $|F| \geq |\mathcal{O}'|$. //

We could, of course, have chosen any set of points, but the vertices represent a convenient set. Unfortunately, it is *not* the case that $|F| = |\mathcal{O}'|$. For Fig. 24 below, $|\mathcal{O}'| = 2$, but $|F| = 3$. However, $|P|$ is an upper bound on $|F|$.

PROPOSITION 2. *Let P be a (possibly nonsimple) polygon with vertices $\mathcal{O} = \{p_1, \dots, p_n\}$. Then $P = \cup_{p_i \in \mathcal{O}} V_{p_i}$. Therefore $|F| \leq |P|$.*

Proof. Any polygon P can be decomposed into its primary convex subsets P_1, P_2, \dots, P_m (see Pavlidis [8]), each of which contains at least one vertex of the polygon. Let $x \in P$. Then, for some P_i , $x \in P_i$. Let p_j be a vertex of P in P_i . Then $x \in V_{p_j}$. Thus $P \subseteq \cup_{p_i \in \mathcal{O}} V_{p_i}$. Since obviously $P \supseteq \cup_{p_i \in \mathcal{O}} V_{p_i}$, the proposition is true. //

FIG. 24. $|\mathcal{O}'| = 2$ but $|F| = 3$.

This proposition shows that the vertices of a polygon form a sufficient set.

In fact, the number of primary convex subsets is equal to the number of concave angles (for P simple), so that $|F| \leq C + 1$ where C is the number of concave angles (see Pavlidis [30]).

Suppose we are given the set of skeleton branch points, $B = \{b_1, \dots, b_n\}$ and their isovists $V_B = \{V_{b_1}, \dots, V_{b_n}\}$. We might attempt to construct a smallest subset, $V_{B'}$, of V_B such that $\bigcup_{b_i \in B'} V_{b_i} = P$. However, this is an instance of the set-cover problem, which is known to be in the class of NP -complete problems (see, e.g., [31]).

Instead, we will describe a suboptimal algorithm to find a subset of B which is sufficient. The algorithm is based on representing the isovists by $(k \times k)$ -long bit vectors. Here, k is chosen to allow for an acceptable scaling of the shape, while keeping the storage costs of the algorithm at a reasonable level. The bit vector is computed by “painting” the interior of an isovist on the array, and then storing the painted array in the bit vector in row major order.

So, let b_{e_1}, \dots, b_{e_n} be the bit vector representations of V_{b_1}, \dots, V_{b_n} , and let b_P be the bit vector representation of the original shape. The algorithm will construct a set $B' = \{b_{i_1}, b_{i_2}, \dots, b_{i_m}\}$ such that $\bigcup_{b_{i_j} \in B'} V_{b_{i_j}} = P$.

- (0) $B' = \phi, j = 0$;
- (1) Let b_l be the element of B with largest area (resolve ties arbitrarily). Set $j = 1$ and $b_{i_1} = b_l$.
- (2) $b_P = b_P - b_{i_j}$. This *set difference* can be efficiently computed using a computer’s basic logical operations. b_P contains the points of P unaccounted for by B' .
- (3) If $b_P = 0$, exit with B' .
- (4) Otherwise, for each $b_i \in B - B'$, compute $b_P \cap b_i$. Let b_k be the bit vector such that $b_P \cap b_k$ has the maximal number of points.
- (5) Set $j = j + 1$, and $b_{i_j} = b_k$.
- (6) Go to 2.

The algorithm can execute step 4 a maximum of n times, since if $B' = B$, then b_P would have been set to 0. Each application of step 4 will require on the order of n bit vector “ands.” Thus, the algorithm requires on the order of n^2 “and” operations and nk^2 storage.

The advantages of using a bit vector representation for the v_{b_i} rather than a list-structure of vertices are:

- (1) The polygon intersections can be computed quickly using the computer’s logical operations, and
- (2) The intersection of two polygons may have many components. Since the descriptions of the individual components are not needed by the algorithm, the bit vector representation is computationally much more convenient.

The disadvantages, of course, are the storage of the bit vectors and the need to possibly scale the shapes to keep the necessary storage within limits. We should point out that there are many special-purpose machines (e.g., CLIP [32]),

PICAP [33]) which could easily support the algorithm using this “iconic” representation.

5. SUMMARY

The notion of an *isovist* was introduced and defined as the set of all points in a polygonal region P visible from a point x in P . This led to consideration of the number of isovists required to “see” the whole region and the definition of *sufficient* and *minimal* sets and paths. *Isovist fields* were defined as the fields of (position-dependent) values of some measure of the shape or size (or other feature) of isovists distributed throughout P .

These basic ideas defined, a technique for computing isovists at given (or all) points in given P 's with arbitrary *barriers* and *holes* was presented. The computation of various scalar fields was outlined and illustrated; these were: the *area*, \mathcal{A} , *perimeter*, \mathcal{B} , *visible perimeter*, $\mathcal{V}\mathcal{P}$, *occlusivity*, \mathcal{O} , and *compactness*, \mathcal{C} , fields, as well as two radial moment fields, *variance*, \mathfrak{M}_2 , and *skewness*, \mathfrak{M}_3 .

Having outlined the nature of isovists and isovist fields, their relevance to the design of buildings was briefly discussed and parallels in computer vision and pattern recognition suggested.

We concluded with a more thorough examination of the problem of computing minimal sets. It was proved that the branch points of the skeleton of a polygon constitute a sufficient, though not necessarily a minimal, set. Propositions as to the upper and lower bounds on the size of a minimal set were proved and a (sub-optimal) algorithm presented that approaches minimality closely.

REFERENCES

1. C. Zahn and R. Roskies, Fourier descriptors for plane, closed curves, *IEEE Trans. Computers* **C-21**, 1972, 269–280.
2. E. Persoon and K. S. Fu, Shape discrimination using Fourier descriptors, *IEEE Trans. Systems, Man, Computers* **SMC-7**, 1977, 170–179.
3. M. K. Hu, Visual pattern recognition by moment invariants, *IRE Trans. IT-8*, 1962, 179–187.
4. T. Pavlidis, Waveform approximation through functional approximation, *IEEE Trans. Computers* **C-22**, 1973, 689–697.
5. T. Pavlidis, Segmentation of plane curves, *IEEE Trans. Computers* **C-23**, 1974, 860–870.
6. L. Davis, Understanding shape. I. Angles and sides, *IEEE Trans. Computers* **C-26**, 1977, 236–242.
7. T. Pavlidis, *A Review of Algorithms for Shape Analysis*, Princeton University, Computer Science TR-216, Sept. 1976.
8. T. Pavlidis, Computer recognition of figures through decomposition, *Inform. Contr.* **14**, 1968, 526–537.
9. L. Davis, Understanding shape. II. Symmetry, *IEEE Trans. Systems, Man, Computers*, **SMC-7**, 1977, 204–212.
10. M. Benedikt, To take hold of space: Isovists and isovist fields, *Environ. and Planning B* **6**, 1979, 47–65.
11. J. J. Gibson, *The Senses Considered as Perceptual Systems*, Houghton Mifflin, Boston, 1966.
12. W. F. Clocksin, Perception of surface slant and edge labels from optical flow: A computational approach, University of Edinburgh DAI Working Paper 33, July 1978.
13. H. Blum, A new model of global brain function, *Perspectives in Biol. and Med.* **10**, 1967, 381–408.
14. J. Pfaltz and A. Rosenfeld, Computer representation of planar regions by their skeletons, *Comm. ACM* **10**, 1967, 119–125.

15. A. Rosenfeld and A. Kak, *Digital Picture Processing*, Academic Press, New York, 1976.
16. M. Shamos, *Problems in Computational Geometry*, Springer-Verlag, Berlin/New York, in press.
17. A. Rosenfeld, Compact figures in digital pictures, *IEEE Trans. Systems, Man, Computers* **SMC-4**, 1974, 221-223.
18. L. Shapiro and R. Haralick, Decomposition of two-dimensional shapes by graph-theoretic clustering, *IEEE Trans. PAMI-1* 1979, 10-19.
19. D. Canter and C. Kenny, The spatial environment, in *Environmental Interaction* (D. Canter, Ed.), pp. 133-140, Int. Universities Press, New York, 1975.
20. I. Altman, *The Environment and Social Behavior*, Brooks-Cole, Monterey, Calif., 1975.
21. R. Sommer, *Personal Space*, Prentice-Hall, Englewood Cliffs, N.J., 1969.
22. O. Newman, *Defensible Space*, Macmillan, New York, 1973.
23. R. Mawbry, Defensible space: A theoretical and empirical appraisal, *Urban Studies* **14**, 1977, 169-179.
24. A. Rapaport and R. Hawkes, The perception of urban complexity, *J. Amer. Inst. Planners*, 1970, 106-111.
25. P. Thiel, Towards an envirotecture, unpublished manuscript, University of Washington.
26. K. Lynch, *Managing the Sense of Region*, M.I.T. Press, Cambridge, Mass., 1976.
27. R. Sommer, *Design Awareness*, Holt, Rinehart & Winston, New York, 1972.
28. G. Gallagher, A computer topographic model for determining intervisibility, in *The Mathematics of Large Scale Simulation* (P. Brook, Ed.), Simulation Council Proceedings, Vol. 2, pp. 3-16, 1972.
29. U. Montanari, Continuous skeletons from digitized images, *J. Assoc. Comput. Mach.* **4**, 1969, 534-549.
30. T. Pavlidis, *Structural Pattern Recognition*, Springer-Verlag, Berlin, 1977.
31. A. Aho, J. Hopcroft, and J. Ullman, *The Design and Analysis of Computer Algorithms*, Addison-Wesley, Reading, Mass., 1974.
32. M. Duff, CLIP 4: A large scale integrated circuit array parallel processor, in *Proceedings, 3rd International Joint Conference on Pattern Recognition, 1972*, pp. 728-732.
33. B. Kruse, A parallel picture processing machine, *IEEE Trans. Computers* **C-22**, 1973, 1075-1087.